Synthesis, Spectroscopic Studies, and Structural Studies of *O,O*-Alkylene Dithiophosphate and *N,N*-Dimethyl and Diethyl Dithiocarbamate Derivatives of Halodimethyltellurium(IV)

John E. Drake,* Layla N. Khasrou, Anil G. Mislankar,† and Raju Ratnani‡

Department of Chemistry and Biochemistry, University of Windsor, Windsor, Ontario, Canada N9B 3P4

Received March 12, 1999

O,O-Alkylene dithiophosphate derivatives of halodimethyltellurium(IV) of the type $Me_2TeX[S_2\overline{POGO}]_2$, where X = Cl, Br, I, G = $-CMe_2CMe_2-$, $-CH_2CMe_2CH_2-$, and $-CH_2CEt_2CH_2-$, were synthesized in 80−90% yields by the reaction in dichloromethane of the appropriate dimethyltellurium dihalide with equimolar amounts of the salt of one of the dithiophosphoric acids. Similarly were prepared related *N,N*-dimethyl and *N,N*-diethyl dithiocarbamates of the type $Me_2TeX[S_2CNR_2]$, where R = Me and Et. The compounds were characterized by elemental analyses, ^1H, ^{13}C, ^{31}P, and ^{125}Te NMR, infrared and Raman spectroscopy, and crystal structures when possible. The crystal structures of $Me_2TeCl[S_2\overline{POCMe_2CMe_2O}]$ (**1**), $Me_2TeI[S_2\overline{POCMe_2CMe_2O}]$ (**3**), $Me_2TeCl[S_2CNEt_2]$ (**10**), $Me_2TeBr[S_2CNEt_2]$ (**13**), $Me_2TeI[S_2CNEt_2]$ (**14**), $Me_2TeBr[S_2COMe]$ (**15**), and Me_2TeBr_2 (**16**) are reported. The immediate environment about tellurium in all molecules is essentially that of a sawhorse structure in which the lone pair is apparently stereochemically active and occupying an equatorial position in a distorted trigonal bipyramid. When secondary intra- and intermolecular interactions are included, alternative descriptions of these solid-state structures may be more appropriate.

Introduction

Several reports on organotellurium(IV) compounds with 1,1-dithio ligands have appeared on *O*-alkyl dithiocarbonates,[1−6] *N,N*-dialkyl dithiocarbamates,[5−14] and *O,O*-dialkyl and alkylene dithiophosphates,[4−6,13−21] but reports on related halo derivatives of the type Me_2TeXL have been limited to a few *N,N*-dialkyl dithiocarbamates,[12] along with more recent reports of $Me_2TeX[S_2COR]$ and $Me_2TeX[S_2CN(CH)_nCH_2]$.[22,23] In attempts to prepare mixed ligand complexes including $Me_2Te[S_2CNR_2][S_2COR]$, $Me_2Te[S_2CNR_2][S_2\overline{POCMe_2CMe_2O}]$, and $Me_2Te[S_2COR][S_2\overline{POCMe_2CMe_2O}]$,[24] the halo derivatives were formed as intermediates; several of these have now been isolated. The synthesis and characterization are reported of *O,O*-alkylene dithiophosphate and dithiocarbamate derivatives of halodimethyltellurium(IV), $Me_2TeX[S_2\overline{POGO}]$, where X = Cl, Br, I, G = $-CMe_2CMe_2-$, $-CH_2CMe_2CH_2-$, and $-CH_2CEt_2CH_2-$, and $Me_2TeX[S_2CNR_2]$, where R = Me, Et. The X-ray crystal structures of $Me_2TeCl[S_2\overline{POCMe_2CMe_2O}]$ (**1**), $Me_2TeI[S_2\overline{POCMe_2CMe_2O}]$ (**3**), $Me_2TeCl[S_2CNEt_2]$ (**10**), $Me_2TeBr[S_2CNEt_2]$ (**13**), and $Me_2TeI[S_2CNEt_2]$ (**14**) are included along with those of $Me_2TeBr[S_2COMe]$ (**15**) and Me_2TeBr_2 (**16**) to provide further comparisons.

Experimental Section

Materials. $TeCl_4$ and Me_4Sn were obtained from Aldrich. $TeBr_4$ and Me_2TeI_2 were obtained from Alpha and Organometallics, Inc., respectively. Me_2TeCl_2 and Me_2TeBr_2 were prepared by the adaption of the method described in the literature for the preparation of Ph_2-

* Author to whom correspondence should be addressed.
† Current address: Information Technology, Celestica Inc., Toronto, ON M3C 1V7, Canada.
‡ Current address: Department of Applied Chemistry & Chemical Technology, M.D.S. University, Ajmer, India.

(1) Wieber, M.; Schmidt, E.; Burschka, C. *Z. Anorg. Allg. Chem.* **1985**, *525*, 127.
(2) Bailey, J. H. E.; Drake, J. E.; Khasrou, L. N.; Yang, J. *Inorg. Chem.* **1995**, *34*, 124.
(3) Singh, A. K.; Basumatary, J. K.; Singh, T. P.; Padmanabhan, B. *J. Organomet. Chem.* **1992**, *424*, 33.
(4) Husebye, S.; Maartmann-Moe, K.; Mikalsen, O. *Acta Chem. Scand.* **1990**, *44*, 464.
(5) Dakternieks, D.; Di Giacomo, R.; Gable, R. W.; Hoskins, B. F. *J. Am. Chem. Soc.* **1988**, *110*, 6753.
(6) Singh, A. K.; Basumatary, J. K. *J. Organomet. Chem.* **1989**, *364*, 73.
(7) Bailey, J. H. E.; Drake, J. E.; Sarkar, A. B.; Wong, M. L. Y. *Can. J. Chem.* **1989**, *67*, 1735.
(8) Bailey, J. H. E.; Drake, J. E.; Wong, M. L. Y. *Can. J. Chem.* **1991**, *69*, 1948.
(9) Drake, J. E.; Wong, M. L. Y. *J. Organomet. Chem.* **1989**, *377*, 43.
(10) Husebye, S.; Maartmann-Moe, K.; Steffenson, W. *Acta Chem. Scand.* **1990**, *44*, 139.
(11) Husebye, S.; Maartmann-Moe, K.; Steffenson, W. *Acta Chem. Scand.* **1990**, *44*, 579.
(12) Bailey, J. H. E.; Drake, J. E. *Can. J. Chem.* **1993**, *71*, 42.
(13) Dakternieks, D.; Di Giacomo, R.; Gable, R. W.; Hoskins, B. F. *J. Organomet. Chem.* **1988**, *349*, 305.
(14) Dakternieks, D.; Di Giacomo, R.; Gable, R. W.; Hoskins, B. F. *J. Am. Chem. Soc.* **1988**, *110*, 6762.
(15) Chadha, R. K.; Drake, J. E.; McManus, N. T.; Quinlan, B. A.; Sarkar, A. B. *Organometallics* **1987**, *6*, 813.
(16) Dakternieks, D.; Di Giacomo, R.; Gable, R. W.; Hoskins, B. F. *J. Am. Chem. Soc.* **1988**, *110*, 6541.
(17) Husebye, S.; Maartmann-Moe, K.; Mikalsen, O. *Acta Chem. Scand.* **1989**, *43*, 868.
(18) Srivastava, T. N.; Singh, J. D.; Srivastava, S. K. *Synth. React. Inorg. Met.-Org. Chem.* **1990**, *20*, 503.
(19) Srivastava, T. N.; Singh, J. D.; Srivastava, S. K. *Phosphorus, Sulfur Silicon Relat. Elem.* **1991**, *55*, 117.
(20) Srivastava, T. N.; Singh, J. D.; Srivastava, S. K. *Polyhedron* **1990**, *9*, 943.
(21) Drake, J. E.; Khasrou, L. N.; Mislankar, A. G.; Ratnani, R. *Can. J. Chem.* **1994**, *72*, 1328.
(22) Drake, J. E.; Drake, R. J.; Khasrou, L. N.; Ratnani, R. *Inorg. Chem.* **1996**, *35*, 2831.
(23) Drake, J. E.; Yang, J. *Inorg. Chem.* **1997**, *36*, 1890.
(24) Drake, J. E.; Khasrou, L. N.; Mislankar, A. G.; Ratnani, R. *Can. J. Chem.* **1999**, *77*, 1262.

10.1021/ic990281f CCC: $18.00
Published on Web 08/21/1999

$TeCl_2$[25] by the reaction of $TeCl_4$ or $TeBr_4$ with Me_4Sn in toluene at 60 °C under reflux for 4 h. Sodium and ammonium salts of alkylene dithiophosphates were prepared by literature methods.[26] Both NaS_2CNMe_2 and NaS_2CNEt_2, obtained from Aldrich as hydrated salts, were dried under vacuum for 4−5 days prior to use. $Me_2TeCl[S_2CNEt_2]$ (**10**) and $Me_2TeBr[S_2COMe]$ (**15**) were prepared as described previously.[12,22] All solvents were dried and distilled prior to use and all reactions carried out under anhydrous conditions.

Preparation of Halodimethyl(*O,O*-alkylene dithiophosphato)-tellurium(IV) Compounds. Typically, $Na[S_2POCMe_2CMe_2O]$ (0.371 g, 1.58 mmol) was added to a solution of Me_2TeCl_2 (0.362 g, 1.58 mmol) in dried CH_2Cl_2 (20 mL). The mixture was stirred for 2 h and then filtered to remove NaCl and unreacted materials. The solvent was reduced to 5 mL under vacuum, *n*-hexane (5 mL) was added, and the solution was left overnight in the refrigerator at −6 °C to crystallize. These were washed with *n*-hexane and dried under vacuum to give $Me_2TeCl[S_2POCMe_2CMe_2O]$ (**1**) as white crystals: 0.533 g, yield 83%, dec 138−141 °C. Anal. Calcd for $C_8H_{18}O_2PS_2ClTe$: C, 23.76; H, 4.48. Found: C, 23.26; H, 4.20. Similarly, by substituting the salts of the two other alkylene dithiophosphate salts, were formed **4** and **7**, as follows. $Me_2TeCl[S_2POCH_2CMe_2CH_2O]$ (**4**) was formed as white crystals: yield 88%, mp 135 °C. Anal. Calcd for $C_7H_{16}O_2PS_2ClTe$: C 21.54, H 4.13. Found: C, 21.36; H, 4.09. $Me_2TeCl[S_2POCH_2CEt_2CH_2O]$ (**7**) was formed as white crystals: yield 84%, mp 112−113 °C. Anal. Calcd for $C_9H_{20}O_2PS_2ClTe$: C, 25.23; H, 4.48. Found: C, 25.28; H, 4.49.

Further, by substituting Me_2TeBr_2 or Me_2TeI_2 as appropriate, were prepared **2**, **3**, **5**, **6**, **8**, and **9**, as follows. $Me_2TeBr[S_2POCMe_2CMe_2O]$ (**2**) was prepared as pale yellow crystals: yield 88%, dec 136−138 °C. Anal. Calcd for $C_8H_{18}O_2PS_2BrTe$: C, 21.04; H, 4.04. Found: C, 20.67; H, 3.99. $Me_2TeBr[S_2POCH_2CMe_2CH_2O]$ (**5**) was prepared as pale yellow crystals: yield 81%, mp 121−123 °C. Anal. Calcd for $C_7H_{16}O_2PS_2BrTe$: C, 19.34; H, 3.71. Found: C, 19.49; H, 3.75. $Me_2TeBr[S_2POCH_2CEt_2CH_2O]$ (**8**) was prepared as pale yellow crystals: yield 87%, mp 106−108 °C. Anal. Calcd for $C_9H_{20}O_2PS_2BrTe$: C, 23.35; H, 4.36. Found: C, 23.41; H, 4.40. $Me_2TeI[S_2POCMe_2CMe_2O]$ (**3**) was prepared as pale yellow crystals: yield 88%, dec 118−121 °C, Anal. Calcd for $C_8H_{18}O_2PS_2ITe$: C, 19.38; H, 3.66. Found: C, 19.25; H, 3.55. $Me_2TeI[S_2POCH_2CMe_2CH_2O]$ (**6**) was prepared as pale yellow crystals: yield 86%, mp 123−126 °C. Anal. Calcd for $C_7H_{16}O_2PS_2ITe$: C, 17.45; H, 3.35. Found: C, 17.28; H, 3.29. $Me_2TeI[S_2POCH_2CEt_2CH_2O]$ (**9**) was prepared as pale yellow crystals: yield 85%, mp 99−100 °C. Anal. Calcd for $C_9H_{20}O_2PS_2ITe$: C, 21.20; H, 3.95. Found: C, 21.16; H, 3.89. Despite extensive efforts in recrystallization, X-ray quality crystals were only obtained for compounds **1** and **3**.

Alternative Syntheses of the Bromo Derivatives. Typically, a slight excess of Me_3SiBr (0.065 mL, 0.42 mmol) was distilled into a solution of $Me_2TeCl[S_2POCMe_2CMe_2O]$ (0.145 g, 0.36 mmol) in CS_2 (20 mL) held at −196 °C. The mixture was then allowed to warm to ambient temperature and stirred for 2 h. The solvent, Me_3SiCl, and Me_3SiBr were slowly evaporated on the vacuum line to give $Me_2TeBr[S_2POCMe_2CMe_2O]$ (**2**): 0.152 g, yield 94%, dec 136−138 °C. $Me_2TeBr[S_2POCH_2CMe_2CH_2O]$ (**5**) and $Me_2TeBr[S_2POCH_2CEt_2CH_2O]$ (**8**) were prepared in the same fashion, but again no X-ray quality crystals were obtained on recrystallization.

Preparation of Bromodimethyl[*N,N*-dialkyl dithiocarbamato]-tellurium(IV) Compounds. Typically, $Na[S_2CNMe_2]$ (0.125 g, 0.87 mmol) was added to a solution of Me_2TeBr_2 (0.277 g, 0.87 mmol) in CH_2Cl_2 (20 mL). The mixture, which immediately changed from colorless to bright yellow, was stirred for 2 h and then filtered to remove NaBr and unreacted materials. The solvent was reduced to 5 mL, *n*-hexane (5 mL) was added, and the solution was left overnight in the refrigerator at −6 °C. Solvent was decanted and the crystals dried under vacuum to give $Me_2TeBr[S_2CNMe_2]$ (**11**) as pale yellow crystals: 0.275 g, yield 88%, dec 136−138 °C. Anal. Calcd for $C_5H_{12}NS_2BrTe$: C,-16.78; N, 3.91; H, 3.38. Found: C, 16.89; N, 4.01; H, 3.47. Similarly starting with $Na[S_2CNEt_2]$ was formed $Me_2TeBr[S_2CNEt_2]$ (**13**) as pale yellow crystals: yield 86%, dec 98−99 °C. Anal. Calcd for $C_7H_{16}NS_2BrTe$: C, 21.79; N, 3.63; H, 4.18. Found: C, 22.91; N, 3.71; H, 4.24.

Preparation of Iododimethyl[*N,N*-dialkyl dithiocarbamato]tellurium(IV) Compounds. Typically, to a solution of Me_2TeI_2 (0.411 g, 1.0 mmol) in CH_2Cl_2 (20 mL) was added $Na[S_2CNMe_2]$ (0.143 g, 1.0 mmol). The colorless solution became yellow-orange within a few minutes of the addition of salt. The reaction mixture was stirred for 2 h and then filtered to remove NaI and unreacted materials. The solvent was pumped off to leave a yellow-orange solid, which was redissolved in CH_2Cl_2 (5 mL), *n*-hexane (5 mL) was added, and the solution was left overnight in the refrigerator at −6 °C. Solvent was decanted and the crystals dried under vacuum to give $Me_2TeI[S_2CNMe_2]$ (**12**) as yellow crystals: 0.365 g, yield 90%, dec 117−119 °C. Anal. Calcd for $C_5H_{12}NS_2ITe$: C, 14.84; N, 3.46; H, 2.99. Found: C, 15.67; N, 3.33; H, 2.97. Similarly was formed $Me_2TeI[S_2CNEt]$ (**14**) as yellow crystals: yield 88%; dec 108−110 °C. Anal. Calcd for $C_7H_{16}NS_2ITe$: C, 19.42; N, 3.23; H, 3.73. Found: C, 20.44; N, 3.30; H, 3.82.

Physical Measurements. Elemental analyses were performed at Guelph Chemical Laboratories, Guelph, Ontario, Canada. The infrared spectra were recorded on a Nicolet 5DX FT spectrometer as CsI pellets, and far-infrared spectra were recorded on a Bomen IR Spectrometer between polyethylene films. The Raman spectra were recorded on a Spectra-Physics 164-spectrometer using the 5145-Å exciting line of an argon ion laser with samples sealed in capillary tubes. The ^1H and ^{13}C NMR spectra were recorded on a Bruker 300 FT/NMR spectrometer in $CDCl_3/C_6D_6$ using Me_4Si as internal standard. The ^{31}P and ^{125}Te NMR spectra were recorded on a Bruker 200 FT/NMR spectrometer in $CDCl_3/C_6D_6$ using H_3PO_4 and Me_2Te as an external standard. The melting points were determined on a Fisher-Johns apparatus.

X-ray Crystallographic Analysis. White platelike crystals of $Me_2TeCl[S_2POCMe_2CMe_2O]$ (**1**), yellow platelike crystals of $Me_2TeI[S_2POCMe_2CMe_2O]$ (**3**), a white block crystal of $Me_2TeCl[S_2CNEt_2]$ (**10**), yellow block crystals of $Me_2TeBr[S_2CNEt_2]$ (**13**), $Me_2TeI[S_2CNEt_2]$ (**14**), and $Me_2TeBr[S_2COMe]$ (**15**), and red block crystals of Me_2TeBr_2 (**16**) were sealed in thin-walled glass capillaries and mounted on a Rigaku AFC6S diffractometer, with graphite-monochromated Mo Kα radiation. The data were collected at a temperature of 23 ± 1 °C using the $\omega-2\theta$ scan technique to a maximum 2θ value of 50.0°. An empirical absorption correction, based on azimuthal scans of several reflections, was applied and the data were corrected for Lorentz and polarization effects.

The structures were solved by direct methods.[27] For **1**, tellurium, sulfur, and Cl(1) were refined anisotropically with the disorder of Cl-(2) successfully modeled with 75% and 25% occupancy for Cl(2a) and Cl(2b), respectively. All of the non-hydrogen atoms were refined anisotropically for **3**, **10**, **13**, and **14**, but only tellurium, bromine, and sulfur for **15** and tellurium and bromine for **16**. The hydrogen atoms were included in their idealized positions with C−H set at 0.95 Å and with isotropic thermal parameters set at 1.2 times that of the carbon atom to which they were attached. The final cycles of full-matrix least-squares refinement[28] were based on 1356 (for **1**), 1487 (for **3**), 1212 (for **10**), 1220 (for **13**), 1450 (for **14**), 491 (for **15**), and 548 (for **16**) observed reflections ($I > 3.00\sigma(I)$) and 157 (for **1**), 136 (for **3**), 109 (for **10**, **13** and **14**), 57 (for **15**), and 36 (for **16**) variable parameters and converged (largest parameter shift was 0.001 times its esd) with

(25) Paul, R. C.; Bhasin, K. K.; Chadha, R. K. *J. Inorg. Nucl. Chem.* **1975**, *37*, 2337.
(26) Chauhan, H. P. S.; Bhasin, C. P.; Srivastava, G.; Mehrotra, R. C. *Phosphorus Sulfur* **1983**, *15*, 99.
(27) Sheldrick, G. M. *Acta Crystallogr. Sect. A* **1990**, *46*, 467.
(28) Least-squares function minimized: $\sum w(|F_o| - |F_c|)^2$, where $w = 4F_o2-(F_o2)$, $\sigma^2(F_o2) = [S^2C + R^2B) + (pF_o2)^2]/(Lp)^2$, S = scan rate, C = total integrated peak count, R = ratio of scan time to background counting time, Lp = Lorentz−polarization factor, and $p = p$ factor.

Table 1. Crystallographic Data for $Me_2TeCl[S_2POCMe_2CMe_2O]$ (**1**), $Me_2TeI[S_2POCMe_2CMe_2O]$ (**3**), $Me_2TeCl[S_2CNEt_2]$ (**10**), $Me_2TeBr[S_2CNEt_2]$ (**13**), $Me_2TeI[S_2CNEt_2]$ (**14**), $Me_2TeBr[S_2COMe]$ (**15**), and Me_2TeBr_2 (**16**)

	1	**3**	**10**	**13**	**14**	**15**	**16**
fw, g mol^{-1}	404.38	495.83	341.38	385.83	432.83	344.74	317.48
a, Å	17.072(1)	12.960(7)	12.239(3)	12.450(4)	9.724(2)	8.47(1)	11.045(5)
b, Å	7.188(8)	11.840(9)	19.255(3)	19.231(2)	11.362(2)	5.950(9)	6.563(5)
c, Å	25.549(2)	20.686(5)	10.984(4)	11.015(3)	12.637(1)	20.65(3)	11.309(6)
β, deg		94.84(3)			97.89(1)	100.5(1)	117.89(4)
V, Å^3	3135(2)	3163(3)	2588(1)	2637(1)	1383.1(3)	1023(3)	724.4(9)
space group	$Pca2_1$	$C2/c$	$Pbca$	$Pbca$	$P2_1/c$	$P2_1/c$	$P2_1/n$
Z	8	8	8	8	4	4	4
ρ_{calcd}, g cm^{-3}	1.71	2.08	1.75	1.94	2.08	2.24	2.91
T, °C	23	23	23	23	23	23	23
μ, cm^{-1}	24.19	41.83	27.85	83.56	46.18	71.19	149.23
R^a	0.0520	0.0578	0.0399	0.0354	0.0373	0.0786	0.0514
$R_w{}^b$	0.0454	0.0479	0.0320	0.0287	0.0328	0.0830	0.0413

[a] $R = \sum||F_o| - |F_c||/\sum|F_o|$. [b] $R_w = [\sum w(|F_o| - |F_c|)^2/\sum wF_o^2)]^{1/2}$, where $w = 1/\sigma^2(F_o)$.

Table 2. Important Interatomic Distances (Å) and Angles (deg) for $Me_2TeCl[S_2POCMe_2CMe_2O]$ (**1**) and $Me_2TeI[S_2POCMe_2CMe_2O]$ (**3**)[a,b]

$Me_2TeCl[S_2POCMe_2CMe_2O]$ (**1**)				$Me_2TeI[S_2POCMe_2CMe_2O]$ (**3**)	
Te(2)−Cl(2a)	2.57(2)	Te(1)−Cl(1)	2.56(1)	Te(1)−I(1)	2.926(2)
Te(2)−Cl(2b)	2.67(2)				
Te(2)−S(3)	2.567(9)	Te(1)−S(1)	2.60(1)	Te(1)−S(1)	2.611(4)
Te(2)−C(9)	2.13(3)	Te(1)−C(1)	2.11(3)	Te(1)−C(1)	2.11(1)
Te(2)−C(10)	2.24(3)	Te(1)−C(2)	2.21(3)	Te(1)−C(2)	2.16(2)
S(3)−P(2)	2.01(1)	S(1)−P(1)	2.08(1)	S(1)−P(1)	2.015(6)
S(4)−P(2)	1.99(1)	S(2)−P(1)	1.88(1)	S(2)−P(1)	1.936(5)
P(2)−O(3)	1.57(2)	P(1)−O(1)	1.59(2)	P(1)−O(1)	1.63(1)
P(2)−O(4)	1.62(3)	P(1)−O(2)	1.62(3)	P(1)−O(2)	1.611(9)
Te(2)- -S(4)	3.39(1)	Te(1)- -S(2)	3.40(1)	Te(1)- -S(2)	3.402(5)
S(3)- -S(4)	3.39(2)	S(1)- -S(2)	3.32(1)	S(1)- -S(2)	3.326(6)
Te(2)- -S(2′)	3.526(7)	Te(1)−S(4)	3.557(7)		
Cl(2a)−Te(2)−S(3)	166.5(4)	Cl(1)−Te(1)−S(1)	164.8(4)	I(1)−Te(1)−S(1)	169.6(1)
Cl(2b)−Te(2)−S(3)	172.1(9)				
Cl(2a)−Te(2)−C(9)	88(1)	Cl(1)−Te(1)−C(1)	85(1)	I(1)−Te(1)−C(1)	85.6(5)
Cl(2b)−Te(2)−C(9)	79(1)				
Cl(2a)−Te(2)−C(10)	81.8(8)	Cl(1)−Te(1)−C(2)	84.4(9)	I(1)−Te(1)−C(2)	86.8(4)
Cl(2b)−Te(2)−C(10)	93(1)				
S(3)−Te(2)−C(9)	94(1)	S(1)−Te(1)−C(1)	87.7(9)	S(1)−Te(1)−C(1)	89.6(5)
S(3)−Te(2)−C(10)	84.7(7)	S(1)−Te(1)−C(2)	83.5(8)	S(1)−Te(1)−C(2)	84.6(4)
C(9)−Te(2)−C(10)	99(1)	C(1)−Te(1)−C(2)	97(1)	C(1)−Te(1)−C(2)	96.8(7)
Te(2)−S(3)−P(2)	99.3(4)	Te(1)−S(1)−P(1)	100.3(4)	Te(1)−S(1)−P(1)	99.9(2)
S(3)−P(2)−S(4)	116.3(6)	S(1)−P(1)−S(2)	113.7(6)	S(1)−P(1)−S(2)	114.7(3)
S(3)−P(2)−O(3)	108.1(8)	S(1)−P(1)−O(1)	102.3(8)	S(1)−P(1)−O(1)	106.0(4)
S(3)−P(2)−O(4)	109.2(7)	S(1)−P(1)−O(2)	105.1(8)	S(1)−P(1)−O(2)	108.0(4)
S(4)−P(2)−O(3)	112.0(9)	S(2)−P(1)−O(1)	122.1(9)	S(2)−P(1)−O(1)	116.7(4)
S(4)−P(2)−O(4)	109.6(7)	S(2)−P(1)−O(2)	117.0(8)	S(2)−P(1)−O(2)	114.1(4)
O(3)−P(2)−O(4)	101(1)	O(1)−P(1)−O(2)	94(1)	O(1)−P(1)−O(2)	95.3(5)
P(2)−O(3)−C(11)	111(2)	P(1)−O(1)−C(3)	112(1)	P(1)−O(1)−C(3)	110.8(8)
P(2)−O(4)−C(14)	108(2)	P(1)−O(2)−C(6)	114(2)	P(1)−O(2)−C(6)	113.3(8)
C(15)−C(14)−C(16)	123(3)	C(7)−C(6)−C(8)	104(2)	C(7)−C(6)−C(8)	115(1)
S(3)−Te(2)- -S(4)	67.9(3)	S(1)−Te(1)- -S(2)	65.6(3)	S(1)−Te(1)- -S(2)	65.6(1)
Cl(2a)−Te(2)- -S(4)	125.5(5)	Cl(1)−Te(1)- -S(2)	125.4(3)	I(1)−Te(1)- -S(2)	122.66(8)
Cl(2b)−Te(2)- -S(4)	114.2(9)				
C(9)−Te(2)- -S(4)	81(1)	C(1)−Te(1)- -S(2)	78.4(9)	C(1)−Te(1)- -S(2)	82.4(4)
C(10)−Te(2)- -S(4)	152.5(7)	C(2)−Te(1)- -S(2)	148.8(9)	C(2)−Te(1)- -S(2)	150.2(4)
Te(2)- -S(2′)−Te(1′)	117.9(3)	Te(1)−S(4)−Te(2)	118.6(3)		

[a] Numbers in parentheses refer to estimated standard deviations in the least-significant digits. [b] Symmetry equivalent position (x, $y - 1$, z) given by prime.

unweighted and weighted agreement factors of $R = \sum|F_o| - |F_c||/\sum|F_o| = 0.0520$ (for **1**), 0.0578 (for **3**), 0.0399 (for **10**), 0.0354 (for **13**), 0.0373 (for **14**), 0.0786 (for **15**), and 0.0514 (for **16**) and $R_w = [(\sum w(|F_o| - |F_c|)^2/\sum wF_o^2)]^{1/2} = 0.0454$ (for **1**), 0.0479 (for **3**), 0.0320 (for **10**), 0.0287 (for **13**), 0.0328 (for **14**), 0.0830 (for **15**), and 0.0413 (for **16**).

The standard deviation of an observation of unit weight[29] was 1.83 (for **1**), 2.26 (for **3**), 1.79 (for **10**), 1.49 (for **13**), 1.42 (for **14**), 2.33 (for **15**), and 1.81 (for **16**). Plots of $\sum w(|F_o| - |F_c|)^2$ vs $|F_o|$, reflection order in data collection, sin θ/λ, and various classes of indices showed no unusual trends. All calculations were performed using the TEXSAN[30] crystallographic software package of Molecular Structure Corp.

Important distances and bond angles are given in Tables 2−4. The molecular structures are displayed as ORTEP diagrams in Figures 1−7. Additional crystallographic data are available as Supporting Information.

(29) Standard deviation of an observation of unit weight: $[\sum w(|F_o| - |F_c|)^2/N_o - N_v)^{1/2}$, where N_o = number of observations and N_v = number of variables.

(30) *TEXSAN-TEXRAY Structure Analysis Package*; Molecular Structure Corp.: Woodlands, TX, 1985.

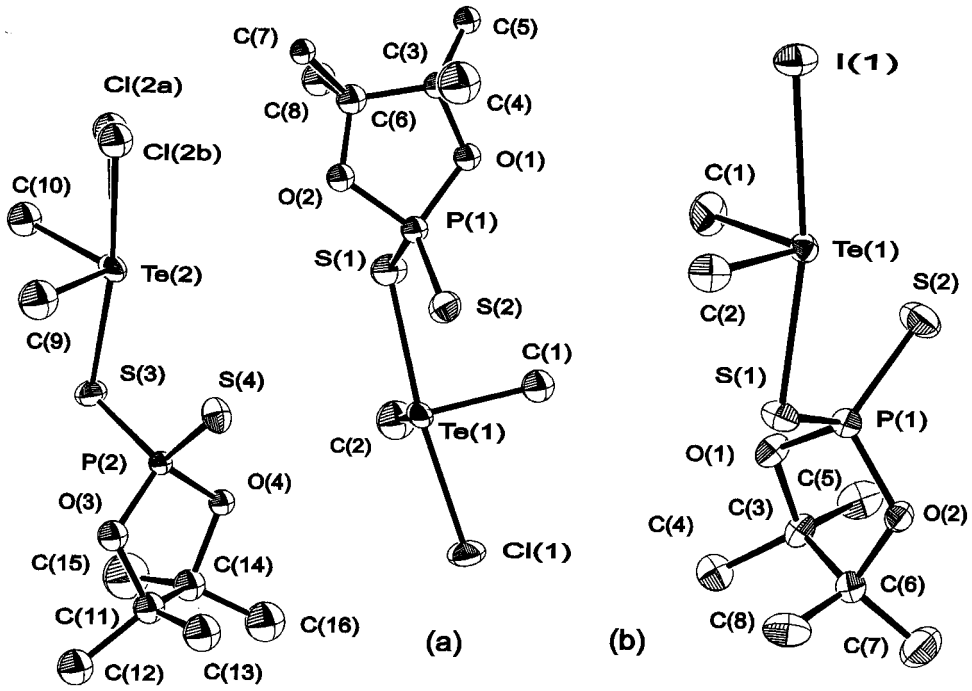

Figure 1. ORTEP plots of the molecules (a) $Me_2TeCl[S_2\overline{POCMe_2CMe_2O}]$ (**1**) showing the two independent molecules in the asymmetric unit and (b) $Me_2TeI[S_2\overline{POCMe_2CMe_2O}]$ (**3**). The atoms are drawn with 30% probability ellipsoids. Hydrogen atoms are omitted for clarity.

Results and Discussion

A number of *O*,*O*-alkylene dithiophosphate derivatives of halodimethyltellurium(IV) are prepared in 80−90% yield by the reaction of dimethyltellurium dichloride, dibromide, or diiodide with the sodium salt of the appropriate *O*,*O*-alkylene dithiophosphoric acid in equimolar ratio in dichloromethane.

$$Me_2TeX_2 + NaS_2\overline{POGO} \rightarrow Me_2TeX[S_2\overline{POGO}] + NaX$$

where X = Cl, Br, I; G = $-CMe_2CMe_2-$, $-CH_2CMe_2CH_2-$, $-CH_2CEt_2CH_2-$.

Alternatively, the chloro derivatives can be essentially quantitatively converted into the bromo derivatives by the action of bromotrimethylsilane in CS_2.

$$Me_2TeCl[S_2\overline{POGO}] + Me_3SiBr \rightarrow Me_2TeBr[S_2\overline{POGO}] + Me_3SiCl$$

The bromo- and iododimethyltellurium(IV) dithiocarbamate compounds **11**−**14** were also obtained in high yields by the reaction of the appropriate dimethyltellurium dihalide with equimolar amounts of the sodium salts of *N*,*N*-dimethyl and *N*,*N*-ethyl dithiocarbamic acids, essentially as described previously for the analogous chloro derivatives.[12]

$$Me_2TeX_2 + NaS_2CNR_2 \rightarrow Me_2TeX[S_2CNR_2]$$

where X = Br, I; R = Me, Et.

Solid samples of all derivatives are found to be stable, at least when stored in the refrigerator, because NMR spectra recorded after several months show no changes from the spectra recorded when the compounds were initially prepared. All compounds are soluble in CH_2Cl_2 and $CHCl_3$ and sparingly soluble in CS_2, C_6H_6, and toluene. However, in solution these compounds slowly decompose; disproportionation to the corresponding dihalide and bis derivative is evident after 1−2 days.

Molecular Structures of $Me_2TeCl[S_2\overline{POCMe_2CMe_2O}]$ (1) and $Me_2TeI[S_2\overline{POCMe_2CMe_2O}]$ (3). The ORTEP diagrams of **1** and **3** (Figure 1) include both molecules in the asymmetric unit in **1**, one of which is disordered. The immediate environment about tellurium is the sawhorse structure typical of tellurium(IV) compounds, at least in the gas phase, in which the lone pair is assumed to be stereochemically active and occupying an equatorial position in a distorted trigonal bipyramid. The two methyl groups occupy the other two equatorial positions with C−Te−C angles close to that reported (96.2(3)°) for $Me_2Te[S_2\overline{POCMe_2CMe_2O}]_2$[21] and with Te−C bond lengths bracketing the value in the bis analogue (2.122(7) Å average). The axial positions are occupied by the halogen atom and one of the sulfur atoms of the dithiophosphate group; the Cl(2)−Te(2)−S(3) angle of 164.8(4)° for the molecule **1** not displaying disorder and the I−Te−S angle of 169.6(1)° in **3** are both slightly more distorted from linear than the S−Te−S angle of 173.26° in $Me_2Te[S_2\overline{POCMe_2CMe_2O}]_2$. The Te−S bonds in **1** (2.58(2) Å average) and **3** (2.611(4) Å) are similar to the shorter of the two Te−S bonds in the analogous bis compound, and only slightly shorter than those in the noncyclic dithiophosphate derivatives, $Ph_2Te[S_2P(OMe)_2]_2$ (2.622(3) Å average)[15] and $Ph_2Te[S_2P(OEt)_2]_2$ (2.615(6) Å average).[13] The Te−X bond lengths (2.60(5) Å average) for Te−Cl and 2.926(2) Å for Te−I) are not very different from the values in Me_2TeCl_2 and Me_2TeI_2 of 2.51(4) and 2.885(3) to 2.994(3) Å, respectively; this point will be readdressed in discussing the $Me_2TeX[S_2CNEt_2]$ species.

As was found for noncyclic dithiophosphates,[13−15] $Me_2Te[S_2\overline{POCMe_2CMe_2O}]_2$, and all related dithio derivatives, the terminal sulfur atoms are oriented toward the tellurium atom at distances (3.397(9) Å average) in **1** and **3** which are well within the sum of the van der Waals radii.[31] The inclusion of the aniso sulfur atom in the coordination sphere leads to square-pyramidal

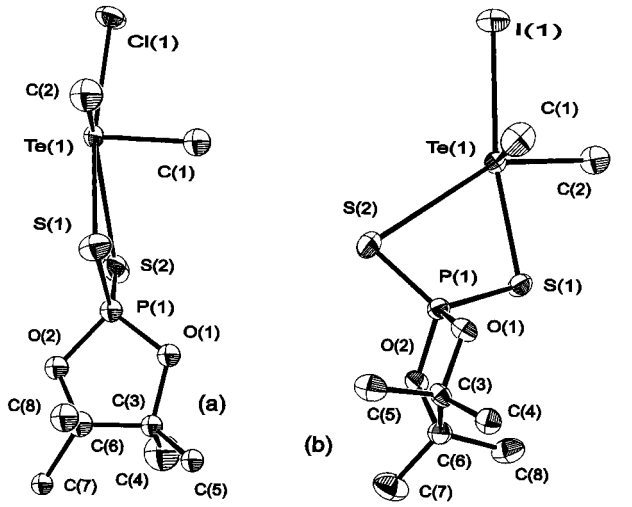

Figure 2. ORTEP plot of the molecules (a) $Me_2TeCl[S_2POCMe_2CMe_2O]$ (**1**) and (b) $Me_2TeI[S_2POCMe_2CMe_2O]$ (**3**) showing the stereochemistry about tellurium when the intramolecular interactions leading to unsymmetrical bidentate ligands are included. The atoms are drawn with 30% probability ellipsoids. Hydrogen atoms are omitted for clarity.

environments about Te (Figure 2) with S−Te- -S bite angles ranging from 65.6(1)° to 67.9(3)° and bite lengths from 3.32-(1) to 3.39(1) Å. The atoms S(1), S(2), Cl(1), C(2) and Te(1) are essentially coplanar (mean deviation from plane is 0.129 Å in **1** and 0.082 Å in **3**) with the second methyl carbon atom C(1) out of the plane by 2.05(3) Å in **1** and 2.05(1) Å in **3**.

The TeS−P bonds are only slightly longer (2.01(1) and 2.08-(1) Å in **1** and 2.015(6) Å in **3**) than the terminal or aniso-bonded P═S bonds (1.99(1) and 1.88(1) Å in **1** and 1.936(5) Å in **3**), lending support to the concept that the aniso S atom is involved in bonding. The remaining bond lengths and angles around phosphorus and those within the ring system are similar to those found in the bis derivative.

There are no internuclear distances in **3** indicating Te- -S′ or Te- -X′ interactions, but in **1**, two are indicated that involve the aniso sulfur atoms; the Te(1)- -S(4) distance of 3.557(7) Å suggesting that the two asymmetric units are linked as dimeric units and the Te(2)- -S(2)′ distance of 3.526(7) Å suggesting that the linking is extended to give a pseudo polymer (see Figure 5a).

Molecular Structures of $Me_2TeCl[S_2CNEt_2]$ (10), $Me_2TeBr[S_2CNEt_2]$ (13), and $Me_2TeI[S_2CNEt_2]$ (14). The ORTEP diagrams in Figure 3 illustrate that in **10**, **13**, and **14** the immediate environment about tellurium is again the typical sawhorse structure with the two methyl groups occupying the other two equatorial positions; the C−Te−C bond angle ranges from 93.7(4) to 95.7(4)°, essentially the same as reported for the related bis derivative, $Me_2Te[S_2CNMe_2]_2$ (93.9(2)°).[12] The average value for the Te−C bond length of 2.12(1) Å is essentially the same as that in $Me_2Te[S_2NCMe_2]_2$ of 2.13(1) Å. The axial positions are again occupied by the halogen atom and by one of the sulfur atoms of the dithiocarbamate group; the X−Te−S bond angle (171.3(5)° average) is closer to linearity than the S−Te−S angle in $Me_2Te[S_2NCMe_2]_2$ (166.5-(15)°), but is essentially identical to the average value of the X−Te−S angle in five related dithioformate derivatives.[23] The Te−S distances in **10**, **13**, and **14** (2.49(1) Å average) are considerably shorter (Table 3) than the distances of 2.654(2) and 2.629(2) Å found for the two Te−S bonds in $Me_2Te[S_2NCMe_2]_2$. By contrast, the Te−X bonds are distinctly longer than in related Me_2TeX_2 species: 2.706(3) Å for Te−Cl in **10** compared to 2.51(4) Å for α-Me_2TeCl_2,[32] 2.883(1) Å for Te−Br in **13** compared to 2.67(4) Å in Me_2TeBr_2, and 3.0997(9) Å for Te−I in **14** compared to a range of 2.885(3) to 2.994(3) Å in α-Me_2TeI_2.[33] The same phenomenon of a shortening of the Te−S bond and lengthening of the Te−X bonds was also noted for the $Me_2TeX[S_2CN(CH_2)_nCH_2]$ analogues and is another example of the trans influence operating on a main group metal. However, this trans influence is virtually nonexistent for $Me_2TeCl[S_2POCMe_2CMe_2O]$ (**1**) and $Me_2TeI[S_2POCMe_2CMe_2O]$ (**3**).

The dithiocarbamate group may also be considered to be an unsymmetrical bidentate ligand by including the Te−S aniso bond in the coordination sphere. These Te(1)- -S(2) bonds in **10**, **13**, and **14**, are also considerably shorter than those in **1** and **3** with distances ranging from 3.136(3) for the iodide to 3.151(3) Å for the chloride compared with an average of 3.397-(9) Å for the dithiophosphates, **1** and **3**. The Te(1)−S(1)−C(3) bond angles are essentially the same in all three derivatives (98.0(3)° average), as are the bite angles (63.1(1)° average), the bite lengths (2.999(2) Å average), and the orientation of the dithiocarbamate group. The atoms S(1), S(2), X(1), C(2), and Te(1) form an approximate plane (mean deviation from plane of 0.069, 0.066 and 0.071 Å for **10**, **13**, and **14**, respectively) with C(1) above the plane (2.09(1), 2.07(2), and 2.06(2) Å for **10**, **13**, and **14**, respectively) to give a distorted square-pyramidal arrangement about tellurium in all three cases. The three molecules are displayed in Figure 4 in slightly different projections to emphasize the pseudo square pyramid.

In contrast to $Me_2TeCl[S_2POCMe_2CMe_2O]$ (**1**) and $Me_2TeI[S_2POCMe_2CMe_2O]$ (**3**), where no intermolecular interactions involving halogen atoms were found, the halogen atoms in **10**, **13**, and **14** form unsymmetrical, essentially rectangular, Te−X- -Te′ bridges with cis Te−X and Te- -X′ bonds within the dimeric species. The Te- -X′ distances of 3.521(4), 3.597(1), and 3.746(1) Å, respectively, for Te- -Cl′, Te- -Br′, and Te- -I′ are marginally longer than those in the three $Me_2TeX[SCONEt_2]$, X = Cl, Br, I, species,[34] similar to those in Me_2TeX_2 species, and shorter than those for $Me_2TeCl[S_2CN(CH_2)_4CH_2]$ and $Me_2TeI[S_2CN(CH_2)_4CH_2]$, where Te- -Cl′ and Te- -I′ are 3.601(6) and 3.872(4), respectively.[23] The inclusion of this interaction in the coordination sphere, along with the stronger intramolecular Te−S interaction, leads to a distorted octahedral environment about tellurium (only **10** is shown in Figure 5b as an example) in which the Te- -X′ bond, rather than a lone pair, is trans to C(1). The C(1)−Te(1)- -Cl′(1), C(1)−Te(1)- -Br′(1), and C(1)−Te(1)- -I′(1) angles of 171.0(3)°, 171.9(3)°, and 173.7(3)°, respectively, have a deviation from linearity of the same order as for the axial X−Te−S system in the basic pseudo trigonal bipyramid.

The values of the TeS(1)−C(3)−S(2) and S(2)−C(3)−N(1) angles (120.5(6)° and 124.2(3)° average, respectively) are consistent with π-bond delocalization within the S_2CN planar moiety being of greater importance in the N−C−S (aniso) and

(31) Bondi, A. J. *Phys. Chem.* **1964**, *68*, 441. Pauling, L. *The Nature of the Chemical Bond, 3rd ed.*; Cornell University Press: Ithaca, NY, 1960; p 260.

(32) Christofferson, G. D.; Sparks, R. A.; McCullough, J. D. *Acta Crystallogr.* **1958**, *11*, 782.

(33) Chan, Y. Y.; Einstein, F. W. B. *J. Chem. Soc., Dalton Trans.* **1972**, 316.

(34) Drake, J. E.; Khasrou, L. N.; Mislankar, A. G.; Ratnani, R. *Inorg. Chem.* **1994**, *33*, 6154.

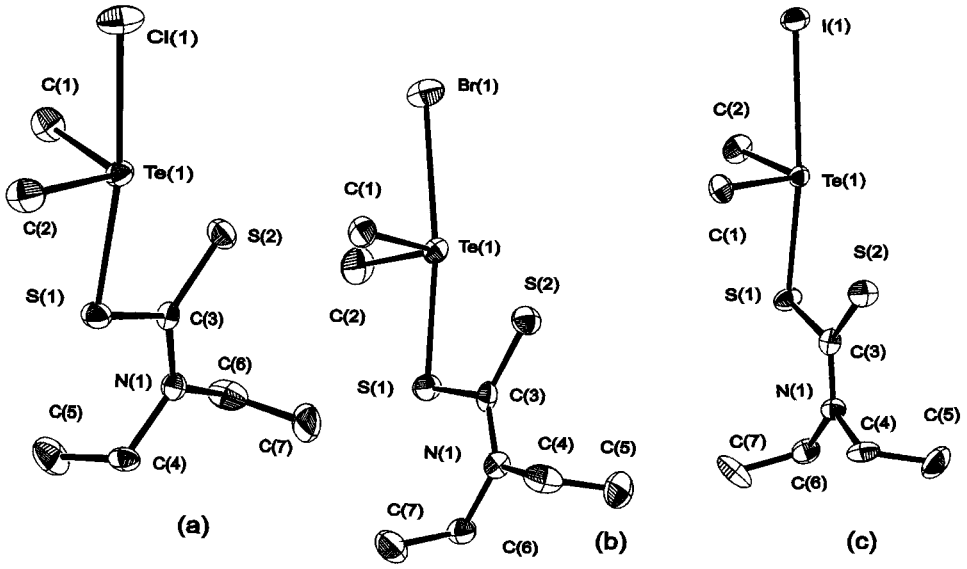

Figure 3. ORTEP plots of the molecules (a) $Me_2TeCl[S_2CNEt_2]$ (**10**), (b) $Me_2TeBr[S_2CNEt_2]$ (**13**), and (c) $Me_2TeI[S_2CNEt_2]$ (**14**). The atoms are drawn with 30% probability ellipsoids. Hydrogen atoms are omitted for clarity.

Table 3. Important Interatomic Distances (Å) and Angles (deg) for $Me_2TeCl[S_2CNEt_2]$ (**10**), $Me_2TeBr[S_2CNEt_2]$ (**13**), and $Me_2TeI[S_2CNEt_2]$ (**14**)

10		**13**		**14**	
Te(1)−Cl(1)	2.706(3)	Te(1)−Br(1)	2.883(1)	Te(1)−I(1)	3.0997(9)
Te(1)−S(1)	2.485(3)	Te(1)−S(1)	2.484(2)	Te(1)−S(1)	2.501(3)
Te(1)−C(1)	2.12(1)	Te(1)−C(1)	2.11(1)	Te(1)−C(1)	2.12(1)
Te(1)−C(2)	2.10(1)	Te(1)−C(2)	2.12(1)	Te(1)−C(2)	2.13(1)
S(1)−C(3)	1.782(9)	S(1)−C(3)	1.772(9)	S(1)−C(3)	1.77(1)
S(2)−C(3)	1.656(9)	S(2)−C(3)	1.69(1)	S(2)−C(3)	1.70(1)
N(1)−C(3)	1.33(1)	N(1)−C(3)	1.32(1)	N(1)−C(3)	1.29(1)
N(1)−C(4)	1.48(1)	N(1)−C(4)	1.49(1)	N(1)−C(4)	1.51(1)
N(1)−C(6)	1.49(1)	N(1)−C(6)	1.47(1)	N(1)−C(6)	1.48(1)
Te(1)- -S(2)	3.151(3)	Te(1)- -S(2)	3.143(3)	Te(1)- -S(2)	3.136(3)
Se(1)- -S(2)	2.998(4)	S(1)- -S(2)	3.000(4)	S(1)- -S(2)	3.001(4)
Te(1)−Cl(1)′	3.521(4)	Te(1)−Br(1)′	3.597(1)	Te(1)−I(1)″	3.746(1)
Te(1)−Te(1)′	4.472(2)	Te(1)−Te(1)′	4.664(2)	Te(1)−Te(1)″	4.886(2)
Cl(1)−Te(1)−S(1)	170.8(1)	Br(1)−Te(1)−S(1)	171.43(7)	I(1)−Te(1)−S(1)	171.70(7)
Cl(1)−Te(1)−C(1)	86.0(3)	Br(1)−Te(1)−C(1)	86.4(3)	I(1)−Te(1)−C(1)	85.6(3)
Cl(1)−Te(1)−C(2)	85.7(3)	Br(1)−Te(1)−C(2)	86.8(3)	I(1)−Te(1)−C(2)	86.4(3)
S(1)−Te(1)−C(1)	91.2(3)	S(1)−Te(1)−C(1)	91.4(3)	S(1)−Te(1)−C(1)	92.6(3)
S(1)−Te(1)−C(2)	85.7(3)	S(1)−Te(1)−C(2)	85.1(3)	S(1)−Te(1)−C(2)	85.7(3)
C(1)−Te(1)−C(2)	93.7(4)	C(1)−Te(1)−C(2)	94.3(4)	C(1)−Te(1)−C(2)	95.7(4)
Te(1)−S(1)−C(3)	97.6(3)	Te(1)−S(1)−C(3)	98.2(3)	Te(1)−S(1)−C(3)	98.3(3)
S(1)−C(3)−S(2)	121.4(6)	S(1)−C(3)−S(2)	120.3(5)	S(1)−C(3)−S(2)	119.7(6)
S(1)−C(3)−N(1)	114.2(7)	S(1)−C(3)−N(1)	115.4(7)	S(1)−C(3)−N(1)	116.5(8)
S(2)−C(3)−N(1)	124.4(7)	S(2)−C(3)−N(1)	124.3(7)	S(2)−C(3)−N(1)	123.8(8)
C(3)−N(1)−C(4)	124.3(8)	C(3)−N(1)−C(4)	120.2(8)	C(3)−N(1)−C(4)	121.2(8)
C(3)−N(1)−C(6)	120.5(8)	C(3)−N(1)−C(6)	124.4(8)	C(3)−N(1)−C(6)	123.8(8)
S(1)−Te(1)- -S(2)	62.98(9)	S(1)−Te(1)- -S(2)	63.18(8)	S(1)−Te(1)- -S(2)	63.16(8)
Cl(1)−Te(1)- -S(2)	125.2(1)	Br(1)−Te(1)- -S(2)	124.62(6)	I(1)−Te(1)- -S(2)	124.44(6)
C(1)−Te(1)- -S(2)	83.8(3)	C(1)−Te(1)- -S(2)	83.4(3)	C(1)−Te(1)- -S(2)	82.1(3)
C(2)−Te(1)- -S(2)	148.5(3)	C(2)−Te(1)- -S(2)	148.0(3)	C(2)−Te(1)- -S(2)	148.6(3)
Cl(1)−Te(1)- -Cl(1)′	88.59(3)	Br(1)−Te(1)- -Br(1)′	88.59(3)	I(1)−Te(1)- -I(1)″	89.41(3)
Te(1)−Cl(1)- -Te(1)′	91.41(3)	Te(1)−Br(1)- -Te(1)′	91.41(3)	Te(1)−I(1)- -Te(1)″	90.59(3)
C(1)−Te(1)- -Cl(1)′	171.0(3)	C(1)−Te(1)- -Br(1)′	!71.9(3)	C(1)−Te(1)- -I(1)″	173.7(3)

[a] Numbers in parentheses refer to estimated standard deviations in the least-significant digits. [b] Symmetry equivalent positions $(1 - x, -y, -z)$ given by prime and $(-x, -y, 1 - z)$ by double prime.

S−C−S bonds. The sum of the three angles about N is 360°, confirming that the nitrogen atom is also planar. The bonding parameters are essentially as expected for anisobidentate dithiocarbamate and monothiocarbamate derivatives.[23,34] Thus the (Te)S−C bonds (1.775(6) Å average) are shorter than the sum of the covalent radii of C and S of 1.81 Å, suggesting a small degree of participation in the delocalized π-bonding, the C−S bond involving the terminal or weakly bonded sulfur atom is longer (1.68(3) Å average) than the C═S bond (ca.1.56 Å) in CS_2, COS, or TeCS,[35] but similar to that in species such as $(NH_2)_2CS$ and thus consistent with a considerable degree of partial π-bond character as well as an anisobidentate link; and the S_2C−N bond length (1.31(2) Å average) is considerably

(35) Wells, A. F. *Structural Inorganic Chemistry*, *4th ed.*; Clarendon Press: Oxford, 1975; p 739.

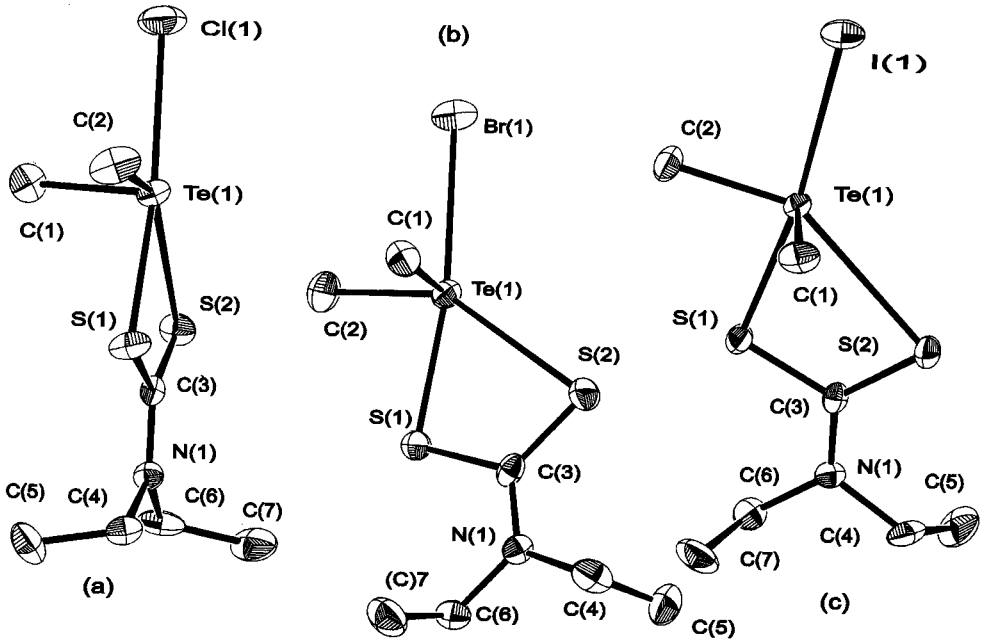

Figure 4. ORTEP plots of the molecules (a) $Me_2TeCl[S_2CNEt_2]$ (**10**), (b) $Me_2TeBr[S_2CNEt_2]$ (**13**), and (c) $Me_2TeI[S_2CNEt_2]$ (**14**) showing the stereochemistry about tellurium when the intramolecular interactions leading to unsymmetrical bidentate ligands are included. The atoms are drawn with 30% probability ellipsoids. Hydrogen atoms are omitted for clarity

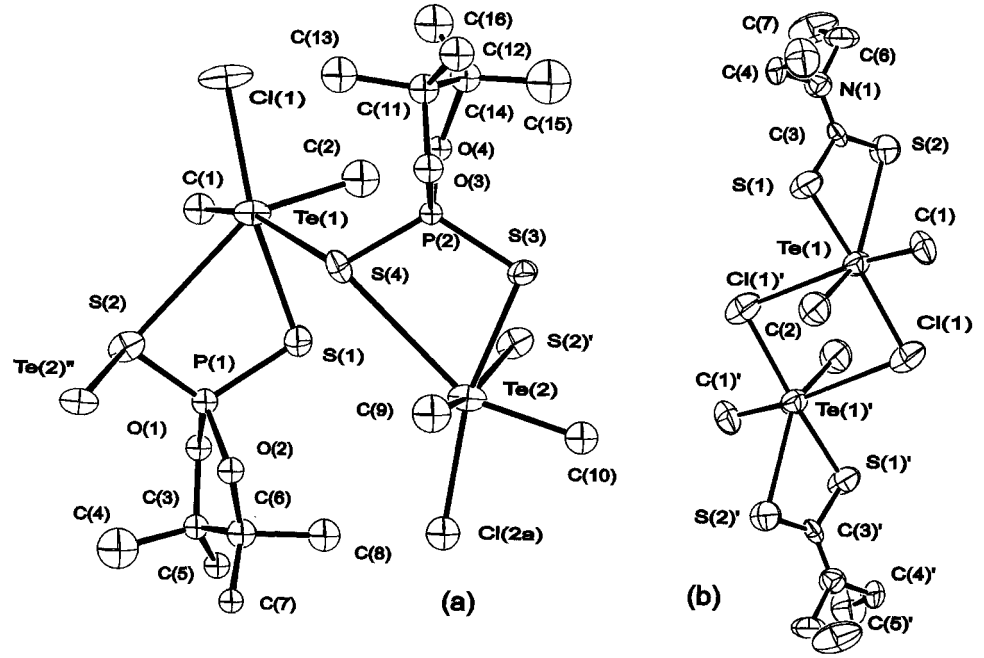

Figure 5. ORTEP plot of the molecules (a) $Me_2TeCl[S_2POCMe_2CMe_2O]$ (**1**) showing weak intermolecular interactions involving the aniso (pendant) sulfur atoms leading to a pseudo dimeric polymer and (b) $Me_2TeCl[S_2CNEt_2]$ (**10**) showing intermolecular interactions involving the chlorine atom leading to a dimer. The atoms are drawn with 30% probability ellipsoids. Hydrogen atoms are omitted for clarity.

shorter than the sum of the covalent radii of C and N of 1.51 Å, confirming that π-electron delocalization extends to the S_2C-N bond.

Molecular Structures of $Me_2TeBr[S_2COMe]$ (15) and Me_2TeBr_2 (16). The ORTEP diagram in Figure 6a illustrates that the immediate environment about tellurium in **15** is again the same sawhorse structure found in the analogous dithiocarbonate derivatives $Me_2TeCl[S_2COEt]$ and $Me_2TeI[S_2CO(i\text{-}Pr)]$[22] as well as **1**, **3**, **10**, **13**, and **14**. The axial Br−Te−S bond angle of 173.3(4)° (Table 4) is close to those in $Me_2TeCl[S_2COEt]$, $Me_2TeI[S_2CO(i\text{-}Pr)]$, and **10**, **13**, and **14**. The Te−S bond (2.53(1) Å) is longer than those in **10**, **13**, and **14** but shorter than those in **1** and **3**, while the Te−Br bond (2.774(7) Å) is shorter than in **13** but longer than in Me_2TeBr_2. Thus the trans influence in $Me_2TeBr[S_2COMe]$ (**15**) is between that in a dithiocarbamate and that in a dithiophosphate, but closer to that in the former.

As with the Te(1)−S(1) bond, the Te(1)- -S(2) aniso bond (3.28(1) Å) in **15**, is again longer than those in **10**, **13**, and **14** but shorter than those in **1** and **3**. The inclusion of this Te−S aniso bond in the coordination sphere results in atoms S(1), S(2), Br(1), C(2), and Te(1) forming an approximate plane (mean deviation from plane of 0.070 Å) with C(1) above the plane (2.09(2) Å) to give the same distorted square-pyramidal arrangement about tellurium as in **10**, **13**, and **14**. The S(1)−

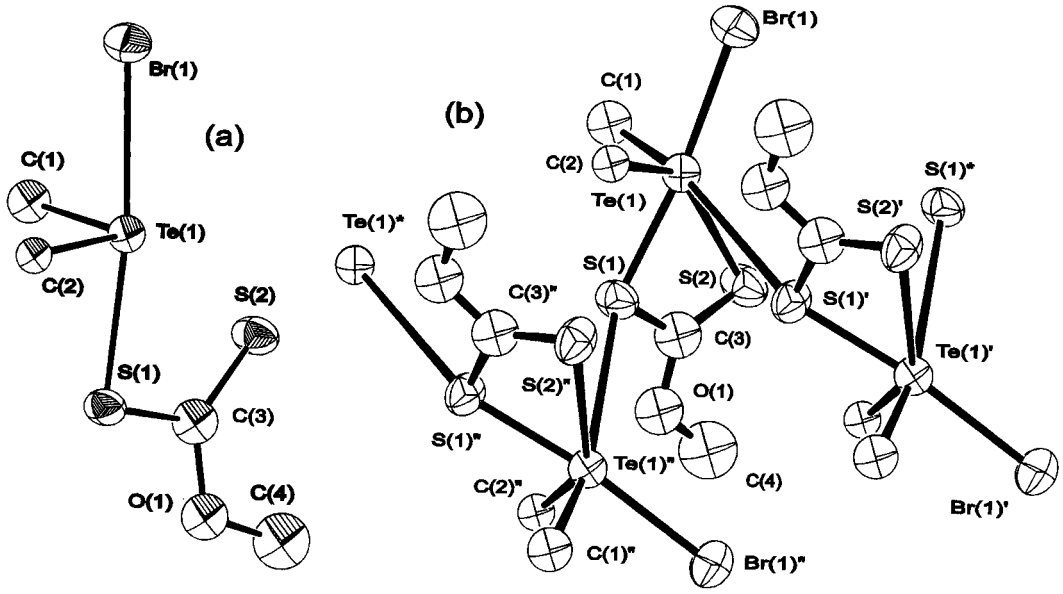

Figure 6. ORTEP plot of the molecule $Me_2TeBr[S_2COMe]$ (**15**) (a) without and (b) with the inclusion of both inter- and intramolecular interactions. The atoms are drawn with 30% probability ellipsoids. Hydrogen atoms are omitted for clarity.

Table 4. Interatomic Distances (Å) and Angles (deg) for $Me_2TeBr[S_2COMe]$ (**15**) and Me_2TeBr_2 (**16**)[a,b]

$Me_2TeBr[S_2COMe]$ (**15**)		Me_2TeBr_2 (**16**)	
Te(1)−Br(1)	2.774(7)	Te(1)−Br(1)	2.622(3)
Te(1)−S(1)	2.53(1)	Te(1)−Br(2)	2.707(3)
Te(1)−C(1)	2.11(5)	Te(1)−C(1)	2.10(2)
Te(1)−C(2)	2.08(5)	Te(1)−C(2)	2.22(2)
S(1)−C(3)	1.73(6)	Te(1)- -Br(2)″	3.562(3)
S(2)−C(3)	1.66(6)	Te(1)- -Br(2)‴	3.660(3)
O(1)−C(3)	1.38(6)		
O(1)−C(4)	1.44(6)		
Te(1)- -S(2)	3.28(1)		
Se(1)- -S(2)	3.01(2)		
Te(1)- -S(1)′	3.61(1)		
Br(1)−Te(1)−S(1)	173.3(4)	Br(1)−Te(1)−Br(2)	173.9(1)
Br(1)−Te(1)−C(1)	86(1)	Br(1)−Te(1)−C(1)	90.6(1)
Br(1)−Te(1)−C(2)	90(1)	Br(1)−Te(1)−C(2)	85.8(5)
S(1)−Te(1)−C(1)	90(1)	Br(2)−Te(1)−C(1)	86.6(6)
S(1)−Te(1)−C(2)	85(1)	Br(2)−Te(1)−C(2)	89.2(5)
C(1)−Te(1)−C(2)	100(2)	C(1)−Te(1)−C(2)	97.4(8)
Te(1)−S(1)−C(3)	98(2)	Br(1)−Te(1)- -Br(2)‴	77.53(8)
S(1)−C(3)−S(2)	125(4)	Te(1)−Br(2)- -Te(1)‴	102.47(8)
S(1)−C(3)−O(1)	108(4)		
S(2)−C(3)−O(1)	126(4)		
C(3)−O(1)−C(4)	115(5)		
S(1)−Te(1)- -S(2)	60.7(4)		
Br(1)−Te(1)- -S(2)	124.8(3)		
C(1)−Te(1)- -S(2)	88(1)		
C(2)−Te(1)- -S(2)	145(1)		
C(1)−Te(1)- -S(1)′	165.2(3)		

[a] Numbers in parentheses refer to estimated standard deviations in the least-significant digits. [b] Symmetry equivalent positions ($1-x, -1/2+y, 3/2-z$) given by prime, ($3/2-x, 1/2+y, 3/2-z$) by double prime, and ($2-x, -y, 2-z$) by triple prime.

Te−S(2) bite angle (60.7(4)°) is essentially the same as in $Me_2TeCl[S_2COEt]$ and $Me_2TeI[S_2CO(i\text{-}Pr)]$,[22] but in contrast to these two analogues in which the former has Te−Cl′ interactions resulting in a pseudo polymer and the latter has Te−I′ interactions resulting in a pseudo dimer, there are no Te(1)−Br(1)′ intermolecular interactions in **15**; the closest such distance is 4.888(8) Å. However, very weak Te(1)- -S(1)′ interactions (3.61(1) Å) appear to give rise to a pseudo dimer (Figure 6b), which is in surprising contrast to the observations for **10**, **13**, and **14**.

The ORTEP diagram in Figure 7a illustrates that the immediate environment about tellurium in dimethyltellurium dibromide (**16**) is again the typical sawhorse structure also reported for $Me_2TeCl_2$32 and Me_2TeI_2.[33] The Br(1)−Te(1)−Br(2) bond angle of 173.9(1) Å can be compared to the corresponding angles in the dichloride and diiodide of 172.3-(3) and 177.3(2) Å, respectively. The Te−Br bonds lengths are not identical, a feature also noted for Me_2TeCl_2 and Me_2TeI_2, and the longer Te(1)−Br(2) bond (2.707(3) Å) is associated with two intermolecular interactions of 3.560(4) and 3.661(4) Å, compared with average Te- -X′ distances of 3.50 and 3.88 Å, respectively, for X = Cl and I. The longer Te- -Br‴ link leads to a bridge resulting in dimers, but unlike **13**, the Br(2)- -Te(1)−Br(2)‴ and Te(1)- -Br(2)- -Te(1)‴ angles are not close to 90° so the bridge is better described as a parallelogram. The shorter Te- -Br″ interaction results in an extended structure (Figure 7b) and the "pseudo dimeric polymer" arrangement is somewhat reminiscent of the effect of the aniso sulfur atoms in **1**.

Infrared and Raman Spectra. Characteristic features of the infrared and Raman spectra of $Me_2TeX[S_2POCMe_2CMe_2O]$ (**1**−**3**), $Me_2TeX[S_2POCH_2CMe_2CH_2O]$ (**4**−**6**), and $Me_2TeX[S_2POCH_2CEt_2CH_2O]$ (**7**−**9**) are summarized in Table 5. The infrared spectra, particularly in the region ca. 600−1200 cm^{-1}, provide useful fingerprint identifications because all of the compounds have distinctive strong bands which are similar, but not identical, to those of the starting salts and corresponding bis derivatives.[21] The similarity of these outstanding features suggests that the bonding within the dithiophosphate groups is essentially unchanged. The asymmetric and symmetric Te−C stretching vibrations are assigned between 540 and 520 cm^{-1} as intense peaks in the Raman spectra. One peak, assignable to the Te−S stretch between 300 and 350 cm^{-1}, is close to the average value for the asymmetric and symmetric stretches in the bis compounds and so is consistent with the Te−S bond being relatively unchanged by halogen substitution. Similarly, the Te−X stretches assigned at ca. 236−249, 145−158, and 110−116 cm^{-1}, respectively, for X = Cl, Br, and I, are close to the average values for the asymmetric and symmetric stretches in the Me_2TeX_2 series[36] and hence consistent with little or no

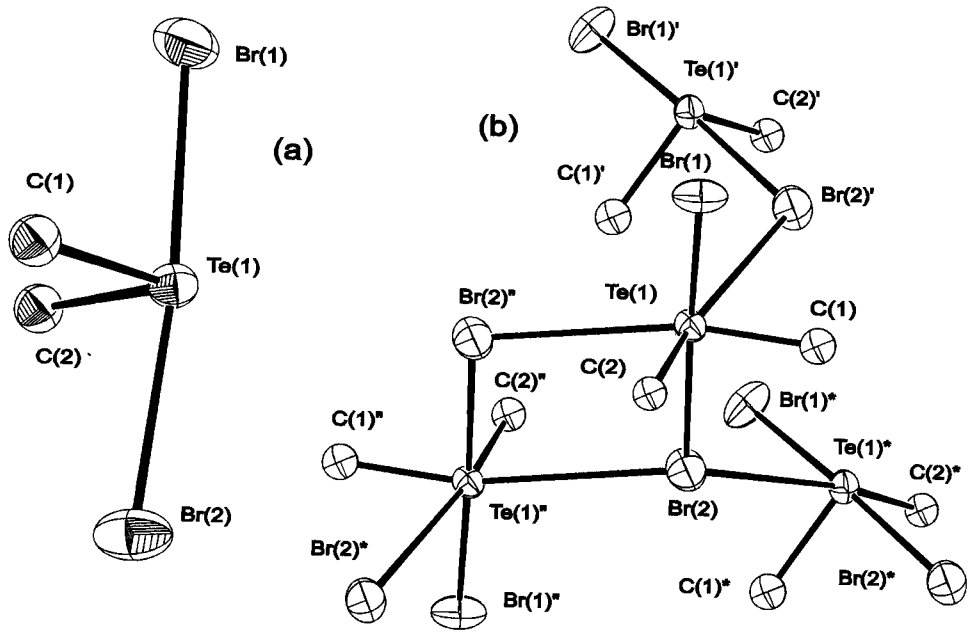

Figure 7. ORTEP plot of the molecule Me_2TeBr_2 (**16**) (a) without and (b) with the inclusion of both intermolecular interactions. The atoms are drawn with 30% probability ellipsoids. Hydrogen atoms are omitted for clarity.

Table 5. Selected Features and Their Assignments in the Vibrational Spectra of Compounds **1**−**9**[a,b]

$Me_2TeX[S_2POCMe_2CMe_2O]$ (**1**−**3**)			$Me_2TeX[S_2POCH_2CMe_2CH_2O]_2$ (**4**−**6**)			$Me_2TeX[S_2POCH_2CEt_2CH_2O]_2$ (**7**−**9**)			
X = Cl (**1**) IR[c] *Raman*[d]	X = Br (**2**) IR[c] *Raman*[d]	X = I (**3**) IR[c] *Raman*[d]	X = Cl (**4**) IR[c] *Raman*[d]	X = Br (**5**) IR[c] *Raman*[d]	X = I (**6**) IR[c] *Raman*[d]	X = Cl (**7**) IR[c] *Raman*[d]	X = Br (**8**) IR[c] *Raman*[d]	X = I (**9**) IR[c]	assignment
1141 ms	1138 ms	1137 m	1047 s	1045 s	1043 s	1069 s	1069 s	1067 ms	$\nu(O-C)_{asym}$
956 ms	954 ms	954 m	988 vs	987 vs	983 vs	1015 s	1015 s	1017 s	$\nu(O-C)_{sym}$
918 vs	921 vs	914 vs	955 s	953 s	947 s	995 s	991 vs	993 s	ν(C−C) ring
857 m	855 s	852 m	913 ms	913 ms	909 ms	938 s	933 s	936 s	$\nu(PO_2)_{asym}$
786 m	782 m	783 m	813 s	812 s	807 s	806 vs	809 vs	806 vs	$\nu(PO_2)_{sym}$
685 s	681 s	686 s	678 vs	678 vs	674 vs	685 vs	679 vs	686 vs	ν(P═S)/$\nu(P-S)_{asym}$
682 (15)		*687 (12)*	*675 (40)*	*676 (45)*	*676 (20)*	*682 (30)*	*671 (40)*	n.o.	
596 s	593 s	590 s	513 s	511 ms	509 ms	522 s	511 ms	521 s	$\nu(P-S)_{sym}$
593 (5)	n.o.	*594 (10)*	*512 (40)*	*511 (30)*	*514 (30)*	n.o.	*517 (85)*	n.o.	
n.o.	n.o.	n.o.	n.o.	n.o.	n.o.	n.o.	n.o.	n.o.	$\nu(Te-C)_{asym}$
540 (100)	*536 (100)*	*531 (60)*	*537 (60)*	*536 (75)*	*530 (30)*	*536 (50)*	*535 (65)*	530 (25)	
n.o	n.o.	n.o.	n.o.	n.o.	n.o.	n.o.	n.o.	n.o.	$\nu(Te-C)_{sym}$
525 (80)	*521 (90)*	*522 (100)*	*528 (100)*	*522 (100)*	*523 (50)*	*524 (100)*	*523 (100)*	522 (40)	
319 m	321 m	303 ms	347 ms	344 ms	339 ms	343 m	341 ms	341 m	ν(Te−S)
313 (35)	*310 (40)*	*300 (90)*	*348 (80)*	*348 (80)*	*348 (40)*	*347 (45)*	*339 (90)*	344 (40)	
243 m	146 mw	116 m	237 m	144 s	110 sh	243 ms	152 m	112 m	ν(Te−X)
236 (20)	*148 (100)*	n.o.	*237 (20)*	*143 (100)*	115 (100)	*249 (60)*	*158 (100)*	114 (100)	

[a] Parentheses denote relative intensities in the Raman effect; peaks with intensities below 10 not included. [b] s = strong, m = medium, w = weak, sh = shoulder, and v = very. [c] Run neat between KBr plates down to 400 cm^{-1} and between polyethylene below 400 cm^{-1}. [d] Run neat in glass capillaries.

weakening of the Te−X bond in contrast to findings for the Me_2TeXL species, where L = $[S_2CN(CH_2)_nCH_2]$[23] and $[SCONEt_2]$.[34]

Characteristic features of the infrared and Raman spectra of $Me_2TeBr[S_2CNMe_2]$ (**11**), $Me_2TeI[S_2CNMe_2]$ (**12**), $Me_2TeBr[S_2CNEt_2]$ (**13**), and Me_2 $TeI[S_2CNEt_2]$ (**14**) are summarized in Table 6. The assignments are based primarily on those reported for *N*,*N*-dialkyl dithiocarbamate derivatives in general and tellurium derivatives in particular,[7,8] as well as the $Me_2TeCl[S_2CNR_2]$[12] and $Me_2TeX[SCONR_2]$[34] analogues. The position of the characteristic C−NR_2 stretching vibration at ca. 1507 cm^{-1} for **11** and **12** and 1492 cm^{-1} for **13** and **14** is much closer to that expected for a C═N double bond (approximately 1600 cm^{-1} for a bond length of 1.27 Å) than for a C−N single bond (approximately 1000 cm^{-1} for a bond length of 1.46 Å), reflecting the significant π-character of the bond and is consistent with the C−N bond length (1.31(2) Å average) found for **10**, **13**, and **14**. The assignment of the C−S (terminal or aniso) stretch at ca. 963 cm^{-1} for **11** and **12** and ca. 980 cm^{-1} for **13** and **14** is in the same range as in related dithiocarbamates[12] and lies between the weighted average (ca. 800 cm^{-1}) of ν(C−S) in the partially double bonded C−S bonds in the CS_3^{2-} ion[37] and the average value (1090 cm^{-1}) for the C═S double bonds in CS_2. This is consistent with partial π-bond character in the C−S terminal or aniso bonds that average 1.68(3) Å.

As with **1**−**9**, the asymmetric and symmetric Te−C stretches are again readily assigned to prominent peaks in close proximity

(36) Hayward, G. C.; Hendra, P. J. *J. Chem. Soc. A* **1969**, 1760.

(37) Ross, S. D. *Inorganic IR and Raman Spectra*; McGraw-Hill; London, 1972; p 160.

Table 6. Selected Features and Their Assignments in the Vibrational Spectra of Compounds **11**−**14**[a,b]

$Me_2TeX[S_2CNMe_2]$ (**11**, **12**)		$Me_2TeX[S_2CNEt_2]$ (**13**, **14**)		
X = Br (**11**) IR[c] *Raman*[d]	X = I (**12**) IR[c] *Raman*[d]	X = Br (**13**) IR[c] *Raman*[d]	X = I (**14**) IR[c] *Raman*[d]	assignment
1508 s	1506 s	1492 s	1491 s	ν(C−NR_2)
965 s	960 s	979 m	979 m	ν(C═S)
966 (15)	*962 (15)*	*985 (15)*	*982 (10)*	
541 mw	526 w,br	529 w,br	510 w,vbr	ν(Te−C)$_{asym}$
537 (100)	*532 (65)*	*533 (75)*	*527 (45)*	
515 w	526 w,br	529 w,br	510 w,vbr	ν(Te−C)$_{sym}$
517 (85)	*514 (50)*	*523 (90)*	*517 (40)*	
384 ms	377 m	395 ms	391 m	ν(Te−S)
383 (90)	*379 (100)*	*393 (100)*	*391 (100)*	
143 ms	104 m	137 m	102 m	ν(Te−X)
140 (40)		*140 (10)*	*110 (15)*	

[a] Parentheses denote relative intensities in the Raman effect; peaks with intensities below 10 not included. [b] s = strong, m = medium, w = weak, v = very, and br = broad. [c] Run neat between KBr plates down to 400 cm^{-1} and between polyethylene below 400 cm^{-1}. [d] Run neat in glass capillaries.

in the Raman spectra between 537 and 514 cm^{-1}. The Te−S stretches in **11**−**14** are assigned to medium-strong peaks in both the Raman and far-infrared spectra in the range 377−395 cm^{-1}, which is consistent with relatively strong Te−S bonds of similar bond length (2.490(9) Å average). In contrast to **1**−**9**, peaks assignable to the Te−X stretch at 208 cm^{-1} for **10** where X = Cl, at 137−143 cm^{-1} for **11** and **13** where X = Br, and at 102−108 cm^{-1} for **12** and **14** where X = I are to lower wavenumbers than in Me_2TeX_2, in which the average values for the symmetric and asymmetric Te−X stretches are 264, 169, and 129 cm^{-1}, respectively for X = Cl, Br, and I.[36] This is consistent with the Te−X bonds being longer and weaker in **10**−**14** than in the dihalides and hence indicative of a strong trans influence.

Nuclear Magnetic Resonance Spectra. The ^{1}H NMR spectral data for $Me_2TeX[S_2\overline{POCMe_2CMe_2O}]$ (**1**−**3**), $Me_2TeX[S_2\overline{POCH_2CMe_2CH_2O}]$ (**4**−**6**), and $Me_2TeX[S_2\overline{POCH_2CEt_2CH_2O}]$ (**7**−**9**) are summarized in Table 7, along with those of ^{13}C, ^{31}P and ^{125}Te NMR. The splitting patterns and intensities of peaks in the ^{1}H NMR spectra taken immediately after dissolution are consistent with the structures of the two compounds **1** and **3** and by extension to the other halo compounds. However, additional peaks corresponding to the increasing presence of Me_2TeX_2, Me_2Te, and the diligand are soon apparent in the spectra, which is consistent with the disproportionation to the bis species followed by its reductive elimination in accord with the equations

$$2Me_2TeX[S_2\overline{POGO}] \rightarrow Me_2TeX_2 + Me_2Te[S_2\overline{POGO}]_2$$

$$Me_2Te[S_2\overline{POGO}]_2 \rightarrow Me_2Te + [S_2\overline{POGO}]_2$$

where X = Cl, Br, I; G = $-CMe_2CMe_2-$, $-CH_2CMe_2CH_2-$, $-CH_2CEt_2CH_2-$.

Similar dissociations in solution are well-established for several diaryltellurium(IV) compounds of the type $R_2Te(S-S)_2$ and $R_2TeX(S-S)$ (where R = C_6H_5, *p*-$MeOC_6H_4$; X = Cl, Br; S−S = *N*,*N*-dialkyl dithiocarbamates).[7,8,12]

The methyl group directly attached to tellurium experiences an upfield shift relative to the corresponding Me_2TeX_2 species as is demonstrated for compounds **1**, **2**, and **3** with chemical shifts of 2.90, 2.93, and 2.96 ppm, respectively, compared to 3.13, 3.26, and 3.27 ppm for Me_2Te-Cl_2, $-Br_2$, and $-I_2$. The similarity of the chemical shift is consistent with all of the compounds having identical links between tellurium and the sulfur atoms of the dithiophosphate groups in solution. The values of the chemical shifts within the dithiophosphate groups are found to be similar to those of the salts from which they were prepared so that, as with the vibrational spectra, there are no significant changes as a result of being linked to tellurium. Despite the fact that the solid-state structures of **1** and **3** show nonequivalent methyl groups substituted on the five-membered ring, only a single peak is observed at ca. 1.43 ppm. The corresponding peak in the salt is also a singlet at 1.46 ppm, so in neither case is the nonequivalence maintained in solution. The α-carbon atoms of the glycoxy groups show equivalent hydrogen atoms on the CH_2 groups in the six-membered ring

Table 7. ^{1}H, ^{13}C, ^{31}P, and ^{125}Te NMR Chemical Shifts for $Me_2TeX[S_2\overline{POCMe_2CMe_2O}]$, X = Cl (**1**), Br (**2**), I (**3**); $Me_2TeX[S_2\overline{POCH_2CMe_2CH_2O}]$, X = Cl (**4**), Br (**5**), I (**6**); and $Me_2TeX[S_2\overline{POCH_2CEt_2CH_2O}]$, X = Cl (**7**), Br (**8**), I (**9**)[a−c]

no.	Te−C*H*$_3$ [Te−*C*H$_3$]	O−C*H*$_2$ [O−*C*]	OC−C*H*$_3$ [OC−C]	OCC−C*H*$_n$ [OCC−*C*]	OCCC−C*H*$_3$ [OCCC−*C*]	^{31}P	^{125}Te
1	2.90 s		1.43 s			103	628
	[22.69 s]	[90.63 s]	[24.32 s]				
2	2.93 s		1.43 s			103.1	599
	[21.64 s]	[90.57 s]	[24.17 d] (J^{PC} 3.8)				
3	2.96 s		1.42 s			104.7	559
	[19.64 s]	[90.42 s]	[24.17 s]				
4	2.95 s	4.03 d (J^{PH} 14.7)		1.06 s		89.7	631
	[22.41 s]	[76.11 s]	[32.14 s]	[21.15 s]			
5	2.99 s	4.03 d (J^{PH} 15.6)		1.05 s		89.8	598
	[24.45 s]	[76.07 d] (J^{PC} 7.4)	[32.15 s]	[21.15 s]			
6	3.01 s	4.02 d (J^{PH} 15.5)		1.05 s		91.5	555
	[19.76 s]	[76.49 s]	[32.53 d] (J^{PC} 5.2)	[21.61 s]			
7	2.95 s	4.09 d (J^{PH} 15.8)		1.45 q (J^{HH} 7.6)	0.84 t (J^{HH} 7.6)	90.7	632
	[22.96 s][d]	[74.07 d] (J^{PC} 7.7)	[37.34 s]	[22.96 s][d]	[7.05 s]		
8	2.98 s	4.09 d (J^{PH} 16.1)		1.45 q (J^{HH} 7.5)	0.83 t (J^{HH} 7.5)	90.8	599
	[21.86 s]	[74.07 d] (J^{PC} 6.3)	[37.34 d] (J^{PC} 3.6)	[22.91 s]	[7.03 s]		
9	2.99 s	4.09 d (J^{PH} 15.8)		1.45 q (J^{HH} 7.5)	0.84 t (J^{HH} 7.5)	92.6	554
	[19.85 s]	[74.95 d] (J^{PC} 8.1)	[37.40 d] (J^{PC} 3.8)	[22.97 s]	[7.06 s]		

[a] The spectra were recorded in $CDCl_3$ and reported in ppm from Me_4Si for ^{1}H and ^{13}C, whose values are given in square brackets, from H_3PO_4 for ^{31}P, and from Me_2Te for ^{125}Te. [b] s = singlet, d = doublet, t = triplet, and q = quartet. [c] Values of coupling constants, in Hz, are given in parentheses. [d] *C*H_3Te and OCC*C* overlap.

Table 8. ^{1}H, $^{13}C\{H\}$, and ^{125}Te NMR Chemical Shifts for $Me_2TeBr[S_2CNMe_2]$ (**11**), $Me_2TeI[S_2CNMe_2]$ (**12**), $Me_2TeBr[S_2CNEt_2]$ (**13**) and $Me_2TeI[S_2CNEt_2]$ (**14**) [a-d]

no.	Te−C*H*$_3$ [Te−*C*H$_3$]	N−C*H*$_n$ [N−*C*]	NC−C*H*$_3$ [NC−*C*]	S−*C*	^{125}Te
11	2.78 s [19.85 s]	3.44 s [44.75 s]		195.5	536
12	2.79 s [18.27 s]	3.45 s [44.76 s]		196	507
13	2.79 s [19.86 s]	3.83 q (J^{HH} = 7.0) [49.31 s]	1.27 t (J^{HH} = 7.0) [12.11 s]	193.5	527
14	2.79 s [18.22 s]	3.83 q (J^{HH} = 7.1) [49.51 s]	1.26 t (J^{HH} = 7.1) [12.25 s]	194	501

[a] The spectra were recorded in $CDCl_3$ and reported in ppm from Me_4Si for ^{1}H and ^{13}C and from Me_2Te for ^{125}Te. [b] s = singlet, t = triplet, and q = quartet. [c] Values of coupling constants, in Hz, are given in parentheses. [d] Corresponding values reported for $Me_2TeCl[S_2CN(CH_3)_2]$ are 2.75 s and [20.5 s] for Te−C*H*$_3$ and [Te−*C*H$_3$], 3.43 s and [44.0 s] for N−C*H*$_3$ and [N−*C*], and 554 for ^{125}Te; for $Me_2TeCl[S_2CN(CH_2CH_3)_2]$ are 2.75 s and [20.4 s] for Te−C*H*$_3$ and [Te−*C*H$_3$], 3.82 q and [49.1 s] for NC*H*$_2$ and [N−*C*], 1.26 t and [12.1 s] for NC−C*H*$_3$ and [NC−*C*], and 545 for ^{125}Te.

centered at ca. 4.03 (for **4**−**6**) and 4.09 ppm (for **7**−**9**). However, as with their starting salts, these peaks appear as doublets arising from coupling with phosphorus with *J*(*PCCH*) ranging from 14.7 to 16.1 Hz. The chemical shifts and coupling constants for **1**−**9** are similar to those reported for other metal complexes in which the linkage of the dithiophosphate groups was assumed to be bidentate.[38]

The $^{31}P\{H\}$ NMR spectral data show a peak for **1**−**9** that is deshielded by about 12.0 ppm, relative to their corresponding free acids. Downfield shifts in the range 8−15 ppm were claimed to be consistent with the presence of bidentate ligands, while negligible shifts or even upfield shifts were associated with monodentate linkages.[39] These values support the presence of bidentate ligands in solution rather than the aniso bidentate linkages found in the solid-state structures. This could be indicative of rapid interchange between the bonding and aniso-bonded sulfur atoms, which could also account for the fact that, as with other bidentate dithiophosphate complexes, there was no sign of the nonequivalence of substituents on the carbon atoms in the ring in either the ^{1}H or ^{13}C NMR spectra, a fact confirmed by recording spectra down to − 90 °C.

In the ^{125}Te NMR spectra peaks are seen at ca. 630 ppm for **1**, **4**, and **7**, at ca. 599 ppm for **2**, **5**, and **8**, and at ca. 555 ppm for **3**, **6**, and **9**, compared to those of the corresponding starting materials Me_2TeCl_2 (734), Me_2TeBr_2 (649), and Me_2TeI_2 (520 ppm) as well as to those of the dithiocarbamate compounds $Me_2TeCl[S_2CNEt_2]$ (**10**) (545 ppm),[12] $Me_2TeBr[S_2CNR]$ (**11** and **13**) (536 and 527 ppm), and $Me_2TeI[S_2CNR]$ (**12** and **14**) (507 and 501 ppm). Thus, the partial substitution of a halide by the $[S_2CNR_2]$ group has a more dramatic effect on the ^{125}Te chemical shift than does the same degree of substitution by the [POGO] group.

The ^{1}H NMR spectral data for $Me_2TeBr[S_2CNMe_2]$ (**11**), $Me_2TeBr[S_2CNEt_2]$ (**13**), $Me_2TeI[S_2CNMe_2]$ (**12**), and $Me_2TeI[S_2CNEt_2]$ (**14**) are given in Table 8, along with those of ^{13}C and ^{125}Te NMR. The splitting patterns and intensities of peaks are consistent with the formulation with the chemical shift of the sharp singlet assignable to the methyl group attached to tellurium in **11**−**14** that is ca. 0.48 ppm upfield from those of the starting materials, compared to ca. 0.18−0.27 for the corresponding dithiophosphates. In the ^{13}C NMR spectra of the iodo derivatives **12** and **14**, the *C*H$_3$−Te peaks appear at ca. 18.25 ppm compared to ca. 19.86 ppm for the bromo derivatives **11** and **13**. This completes the series with ca. 20.5 ppm reported for $Me_2TeCl[S_2CNMe_2]$ and $Me_2TeCl[S_2CNEt_2]$, respectively, indicating a steady downfield shift as the electronegativity of the halogen substituent increases. Peaks for the alkyl groups of the dithiocarbamate entities are found at expected positions compared to the chlorine-substituted analogues,[12] with very weak peaks in the region 193−196 ppm corresponding to S_2CN.

Conclusion

The isolation and spectroscopic characterization of a number of Me_2TeXL species are achieved despite the propensity for such species, particularly the cyclic dithiophosphate derivatives (**1**−**9**), to undergo disproportionation and reductive elimination in solution. The crystal structures confirm that these are not just fortuitous 1:1 mixtures of Me_2TeL_2 and Me_2TeX_2. There are surprising differences in intermolecular interactions given that all of the structures show the same intramolecular associations resulting in aniso bidentate ligands. All three $Me_2TeX[S_2CNEt_2]$ derivatives, X = Cl, Br, I, form pseudo dimers with the rectangular Te−X- -Te′ bridges (Figure 5b), whereas in $Me_2TeCl[S_2POCMe_2CMe_2O]$ the aniso (pendant) sulfur atoms form S- -Te′ links that lead to a pseudo polymer (Figure 5a). By contrast, in $Me_2TeI[S_2POCMe_2CMe_2O]$ there are no similar intermolecular interactions involving halogen or sulfur atoms. Despite the presence of halogen bridging in the dithiocarbamates and the extensive Te−Br- -Te′ links in Me_2TeBr_2 (Figure 7b), there are no intermolecular interactions involving bromine in the apparently structurally similar $Me_2TeBr[S_2COMe]$. Neither are there linkages involving the pendant sulfur atom, but rather there are weak Te−S- -Te′ interactions involving the sulfur atom of the primary Te−S bond (Figure 6b). Finally, the trans influence and the relative strengths of the primary and secondary bonds in the aniso bidentate ligands appear to decrease in the order $Me_2TeX[S_2CNR_2]$ > $Me_2TeX[S_2COR]$ > $Me_2TeX[S_2POCMe_2CMe_2O]$.

Acknowledgment. We thank the Natural Sciences and Engineering Research Council of Canada for financial support and for an NSERC Research Reorientation Associateship for L.N.K.

Supporting Information Available: Table S1−S26 listing experimental details, final atomic coordinates and equivalent isotropic thermal parameters for the non-hydrogen atoms, final fractional coordinates and thermal parameters of hydrogen atoms, anisotropic thermal parameters for selected non-hydrogen atoms, and complete bond distances and angles. This material is available free of charge via the Internet at http://pubs.acs.org. Structure factors may be obtained directly from the authors.

IC990281F

(38) Pandey, S.; Srivastava, G.; Mehrotra, R. C. *Transition Met. Chem.* **1991**, *16*, 252. Ratnani, R.; Srivastava, G.; Mehrotra, R. C. *Transition Met. Chem.* **1991**, *16*, 204. Ratnani, R.; Srivastava, G.; Mehrotra, R. C. *Inorg. Chim. Acta*, **1989**, *161*, 253. Rao, R. J.; Srivastava, G.; Mehrotra, R. C.; Saraswat, B. S.; Mason, J. *Polyhedron* **1984**, *3*, 485.
(39) Glidewell, C. *Inorg. Chim. Acta* **1977**, *25*, 159.